

Courtesy of Julie Arnold and Paula Echeverri. Used with permission.

**16.622 FINAL REPORT**

**EXPANDING FOAM IMPACT ATTENUATION FOR SMALL PARAFOIL  
PAYLOAD PACKAGES**

**MASSACHUSETTS INSTITUTE OF TECHNOLOGY  
DEPARTMENT OF AERONAUTICS AND ASTRONAUTICS  
DECEMBER 9TH, 2003**

**JULIE ARNOLD  
PAULA ECHEVERRI**

**PROJECT ADVISOR: CHRISTIAN ANDERSON**

## Abstract

This project studied expanding foam as a possible mechanism to attenuate the impact of small payloads deployed from unmanned aerial vehicles (UAVs). Current mechanisms, such as paper honeycomb, occupy a significant volumetric fraction of UAV payload capacity. Hypotheses were formulated regarding the performance of expanding foam as compared to honeycomb using the metrics: crush thickness efficiency, pre-deployment volume, and foam expansion reliability. These metrics were evaluated for a payload with a vertical descent rate of 13.5 feet per second and a 50g impact shock limit. The experiment concluded that the crush efficiency of expanding foam is at least 72.7% of the crush efficiency of paper honeycomb, thus proving the hypothesis regarding crush efficiency. The expanding foam is 83% reliable, with 95% confidence, to expand to its expected volume within 30 seconds, thus disproving the hypothesis regarding foam expansion reliability. The pre-deployment volume of expanding foam is at most 33.6% the pre-deployment volume of paper honeycomb; however the hypothesis regarding pre-deployment volume was not assessed within experimental error. Other findings provide insight into the behavior of expanding foam and honeycomb during impact.

## TABLE OF CONTENTS

<b>1. INTRODUCTION.....</b>	<b>8</b>
<b>1.1. BACKGROUND AND MOTIVATION.....</b>	<b>8</b>
<b>1.2. SHORT OVERVIEW OF PROJECT .....</b>	<b>8</b>
<b>1.3. HYPOTHESIS .....</b>	<b>9</b>
<b>1.4. OBJECTIVE .....</b>	<b>9</b>
<b>1.5. SUCCESS CRITERIA .....</b>	<b>9</b>
<b>1.6. OBJECTIVES MET.....</b>	<b>9</b>
<b>2. LITERATURE REVIEW.....</b>	<b>10</b>
<b>3. DESCRIPTION OF EXPERIMENT .....</b>	<b>12</b>
<b>3.1. EXPERIMENT OVERVIEW .....</b>	<b>12</b>
<b>3.2. APPARATUS .....</b>	<b>13</b>
3.2.1. <i>TEST SETUPS.....</i>	<i>13</i>
3.2.2. <i>INSTRUMENTATION.....</i>	<i>15</i>
<b>3.3. TEST ARTICLES .....</b>	<b>16</b>
3.3.1. <i>PAPER HONEYCOMB.....</i>	<i>16</i>
3.3.2. <i>EXPANDING FOAM .....</i>	<i>17</i>
3.3.3. <i>PAYLOAD BOX.....</i>	<i>17</i>
<b>4. DESCRIPTION OF TESTS .....</b>	<b>18</b>
<b>4.1. CRUSH EFFICIENCY .....</b>	<b>18</b>
4.1.1. <i>SCOPE .....</i>	<i>18</i>
4.1.2. <i>METHODS.....</i>	<i>19</i>
4.1.3. <i>CALIBRATION AND ERROR MITIGATION .....</i>	<i>19</i>
4.1.4. <i>TEST MATRICES.....</i>	<i>20</i>
<b>4.2. SAFETY MARGIN .....</b>	<b>21</b>
4.2.1. <i>SCOPE .....</i>	<i>21</i>
4.2.2. <i>METHODS.....</i>	<i>22</i>
4.2.3. <i>CALIBRATION AND ERROR MITIGATION .....</i>	<i>22</i>
4.2.4. <i>TEST MATRIX .....</i>	<i>23</i>
<b>4.3. VOLUME .....</b>	<b>23</b>

4.3.1. SCOPE .....	23
4.3.2. METHODS .....	23
4.3.3. CALIBRATION AND ERROR MITIGATION .....	24
4.3.4. TEST MATRIX .....	24
<b>4.4. FOAM EXPANSION RELIABILITY .....</b>	<b>24</b>
4.4.1. SCOPE .....	24
4.4.2. METHODS .....	25
4.4.3. CALIBRATION AND ERROR MITIGATION .....	25
4.4.4. TEST MATRIX .....	25
<b>5. RESULTS .....</b>	<b>25</b>
<b>6. ANALYSIS OF RESULTS .....</b>	<b>27</b>
<b>6.1. ANALYSIS OF HONEYCOMB CRUSH EFFICIENCY TESTS.....</b>	<b>27</b>
6.1.1. DATA REDUCTION .....	27
6.1.2. DISCUSSION OF RESULTS.....	27
6.1.3. CRUSH THICKNESS EFFICIENCY.....	28
<b>6.2. ANALYSIS OF EXPANDING FOAM CRUSH EFFICIENCY TESTS .....</b>	<b>29</b>
6.2.1. DATA REDUCTION .....	29
6.2.2. DISCUSSION OF RESULTS.....	29
6.2.3. CRUSH THICKNESS EFFICIENCY.....	29
<b>6.3. ANALYSIS OF PAPER HONEYCOMB SAFETY MARGIN TESTS.....</b>	<b>30</b>
6.3.1. DATA REDUCTION .....	30
6.3.2. DATA FILTERING.....	31
6.3.3. DISCUSSION OF RESULTS: COMPARISON TO PREVIOUS THEORY.....	32
6.3.4. SAFETY MARGIN.....	34
<b>6.4. ANALYSIS OF EXPANDING FOAM SAFETY MARGIN TESTS.....</b>	<b>34</b>
6.4.1. ANALYSIS OF EXPANDING FOAM CRUSH STRESS: COMPARISON TO PREVIOUS THEORY .....	34
6.4.2. DATA REDUCTION .....	35
6.4.3. DISCUSSION OF RESULTS.....	36
6.4.4. SAFETY MARGIN.....	37
<b>6.5. VOLUME CALCULATION .....</b>	<b>37</b>

6.5.1. <i>PAPER HONEYCOMB</i> .....	37
6.5.2. <i>EXPANDING FOAM</i> .....	38
<b>6.6. EXPANDING FOAM RELIABILITY TESTS</b> .....	<b>38</b>
<b>6.7. ERROR ANALYSIS</b> .....	<b>38</b>
6.7.1. <i>QUASI-STATIC CRUSH EFFICIENCY ERROR</i> .....	38
6.7.2. <i>PRE-DEPLOYMENT ATTENUATOR VOLUME</i> .....	39
<b>6.8. RELATION OF RESULTS TO HYPOTHESIS</b> .....	<b>43</b>
6.8.1. <i>CRUSH EFFICIENCY</i> .....	43
6.8.2. <i>PRE-DEPLOYMENT VOLUME</i> .....	44
6.8.3. <i>FOAM EXPANSION RELIABILITY</i> .....	44
<b>7. CONCLUSIONS</b> .....	<b>44</b>
7.1. <b>ASSESSMENT OF HYPOTHESIS</b> .....	<b>44</b>
7.2. <b>OTHER FINDINGS</b> .....	<b>44</b>
7.3. <b>SUGGESTIONS FOR FUTURE WORK</b> .....	<b>45</b>
<b>8. REFERENCES</b> .....	<b>52</b>

**APPENDIX A: SELECTIONS OF ANDERSON’S UNPUBLISHED PAPER**

**APPENDIX B: MATLAB CODE FOR SAFETY MARGIN TESTS DATA REDUCTION**

**APPENDIX C: SAFETY MARGIN CONFIDENCE ANALYSIS**

**APPENDIX D: SUMMARY OF INTERMEDIATE RESULTS**

## TABLE OF FIGURES

FIGURE 1: INSTAPAK EXPANDING FOAM.....	9
FIGURE 2: EXPERIMENT OVERVIEW FLOWCHART .....	12
FIGURE 3: DROP-TEST RIG .....	14
FIGURE 4: INSTAPAK QUICK WARMER.....	15
FIGURE 5: SLICED 1-INCH HONEYCOMB.....	16
FIGURE 6: FOAM EXPANSION PROCEDURE .....	17
FIGURE 7: (A) PAYLOAD BOX, (B) TOP VIEW OF PAYLOAD ATTACHED TO DROP-TEST RIG .....	18
FIGURE 8: CONCEPTUAL STRESS VS. DISPLACEMENT CURVE .....	19
FIGURE 9: RESULTS OF EXPANDING FOAM COMPARISON TO PAPER HONEYCOMB.....	26
FIGURE 10:EXAMPLE OF MAXIMUM CRUSH DISPLACEMENT .....	27
FIGURE 11: HONEYCOMB CRUSH THICKNESS EFFICIENCY RESULTS.....	28
FIGURE 12: EXPANDING FOAM CRUSH THICKNESS EFFICIENCY RESULTS .....	29
FIGURE 13: HONEYCOMB DISTRIBUTION OF PEAK ACCELERATIONS.....	31
FIGURE 14: SAMPLE OF FILTERED HONEYCOMB SAFETY MARGIN TRIAL.....	32
FIGURE 15: SAMPLE OF 1-INCH HONEYCOMB QUASI-STATIC LOADING TEST.....	33
FIGURE 16: HONEYCOMB DISTRIBUTION OF SECONDARY PEAK ACCELERATIONS.....	33
FIGURE 17: SAMPLE OF 1-INCH QUASI-STATIC LOADING TEST .....	35
FIGURE 18: EXPANDING FOAM DISTRIBUTION OF PEAK ACCELERATIONS .....	36
FIGURE 19: PRE-DEPLOYMENT VOLUME OF ATTENUATION MATERIAL VS. MAXIMUM ACCELERATION DURING IMPACT .....	45

## LIST OF TABLES

TABLE 1: QUASI-STATIC CRUSH EFFICIENCY TEST MATRICES .....	21
TABLE 2: DYNAMIC CRUSH EFFICIENCY TEST MATRIX .....	21
TABLE 3: SAFETY MARGIN TEST MATRIX.....	23
TABLE 4: VOLUME TEST MATRIX .....	24
TABLE 5: FOAM EXPANSION RELIABILITY TEST MATRIX .....	25

# **1. Introduction**

## **1.1. Background and Motivation**

Delivery of small payloads is one of many concepts currently under development to enhance the functionality of Unmanned Aerial Vehicles (UAVs). UAVs are remotely piloted or autonomous aircraft that can carry cameras, sensors, communications equipment or other payloads, and have been used in reconnaissance and intelligence-gathering since the 1950's. Small parafoils, deployed when payloads are released from UAVs, are a promising delivery method for such payloads and typically show a deployed payload's vertical descent rate of approximately 15 feet per second. A shock absorption mechanism is then often necessary to attenuate the impact shock at touchdown.

Current inexpensive and reliable low-impact attenuators such as paper honeycomb and crushable foam occupy a significant fraction of the volumetric capacity of UAV payload compartments. More complex impact attenuators such as deployable airbags and retractable mechanisms occupy less pre-deployment UAV payload volume. Yet, they greatly increase cost and/or compromise reliability. A new impact attenuation concept that reduces pre-deployment UAV payload volume without significantly increasing cost or reducing reliability is therefore desirable. An expanding foam impact attenuation device may serve this purpose.

## **1.2. Short Overview of Project**

This project involved a series of experiments to assess whether expanding foam could provide efficient and reliable impact attenuation and occupy a minimal volume onboard the UAV. This assessment was conducted by quantitatively comparing the characteristics of expanding foam and honeycomb relevant to deploying small packages from UAVs. Instapak® (Figure 1), a commercially available expanding foam product manufactured by SealedAir Corporation was compared to a paper honeycomb product manufactured by Pactiv Corporation. Products such as Instapak expanding foam and Pactive paper honeycomb are used to protect delicate items in shipping containers from impact shock.



Figure 1: Instapak Expanding Foam

### **1.3. Hypothesis**

The primary hypothesis stated that the pre-deployment volume of an expanding foam impact attenuation device would occupy at most 25% of the volume occupied by paper honeycomb, and that the material would have a crush thickness efficiency of at least 70% of the corresponding value for paper honeycomb. The secondary hypothesis stated that an expanding foam deployment device would cost at most 50% more than paper honeycomb and have a deployment reliability of at least 90% of the corresponding value for paper honeycomb.

### **1.4. Objective**

Assess the ability of expanding foam to protect a payload having a 50 g-impact shock limit from a 15 feet per second vertical descent rate. This assessment was conducted by comparing the pre-deployment volume, crush efficiency, cost and reliability of expanding foam against paper honeycomb.

### **1.5. Success Criteria**

Evaluate the aforementioned metrics for expanding foam and paper honeycomb to an accuracy such that the hypotheses can be assessed.

### **1.6. Objectives Met**

An impact velocity of 15 feet per second could not be achieved consistently during the experiment. Instead, the experiment was conducted for an impact velocity of  $13.5 \pm 0.3$  feet per second.

The hypotheses regarding attenuator efficiency and deployment reliability were assessed within experimental error; however, the hypothesis regarding pre-deployment volume could not be proved or disproved. This experiment confirmed that the crush

efficiency of expanding foam is at least 70% of the crush efficiency of paper honeycomb, and disproved the hypothesis that the foam expansion reliability is at least 90%.

## **2. Literature Review**

Although there does not appear to be previous research investigating the use of an expanding foam material to attenuate the impact of objects deployed from aerial vehicles, there is a great body of literature laying the foundation for such a research experiment. This literature includes various experiments employing standard shock impact testing methodologies, and one resource discussing the use of honeycomb material to attenuate the impact of small payloads deployed from UAVs.

The paper entitled “Design and Testing of the HOPE-X HSFD-II Landing System” written by Gardiner<sup>1</sup> discusses the design, analysis and preliminary testing of the airbag impact attenuation system for the re-entry of the unmanned space vehicle. The paper describes the technical design of the parachute and airbag subsystems, including materials, construction, and deployment techniques. Simulation tools are used to analyze parachute performance, and simulate airbag performance during impact. Airbag drop testing is then performed to validate the simulations. Drop tests include both vertical and horizontal impact velocity components controlled using a rail system. Test output data includes 3-axis acceleration, airbag pressure, rotational rate, vent release monitoring, and high-speed video, and all data is recorded digitally at 1000Hz bandwidth. Gardiner found that drop tests verified computer simulations, and computer simulations were then used to evaluate multiple airbag configurations.

The design and testing of the HOPE-X landing system is primarily focused on simulation verification. Although this aspect of the paper was not useful in designing our impact attenuation experiment, the HOPE-X landing system drop test experiment design provides a baseline with which to design a drop-test rig. Our impact attenuation experiment was constrained to studying the effect of a vertical impact, and so we were not interested in rotational rates. However, a railing system to control the drop, an accelerometer, and a high-speed camera were incorporated into our experiment. Also, the

1000Hz bandwidth requirement provided a useful guideline for the selection of a data acquisition module.

Another paper entitled, “Parachute Retraction Soft-Landing Systems Using Pneumatic Muscle Actuators” written by Brown and Haggard<sup>2</sup> discusses the analysis and testing of flexible composite technology actuators. The actuators contract in the moments before impact to significantly slow the descent of a payload under a parachute. Brown and Haggard derive a theoretical model for the tension in an ideal actuator as a function of contraction, and use static testing to determine the validity of their model. Static testing also provides a measure of the efficiency for the real actuators. Dynamic drop-tests are then conducted to demonstrate the payload velocity reduction due to retraction. The drop-test setup involves placing a load cell between the payload and retraction actuator, and deriving peak force, peak acceleration, and change in velocity from the force versus time data.

While the actual parachute retraction system is not relevant to our project, this work echoes the drop-test methodology laid out in the design and testing of the HOPE-X landing system. Although we intended to use an accelerometer rather than a load cell to record behavior during impact, this paper verifies that initial impact velocity of the payload can be successfully extracted from the impact data. Also, this paper distinguishes between static and dynamic testing. We determined an actual attenuation efficiency using static testing and verified performance through dynamic testing as this paper describes.

Christian Anderson at Draper laboratories has also provided a very relevant paper entitled, “Impact Shock Attenuation for Parafoil Payloads”.<sup>\*</sup> Anderson’s work is the only available resource studying impact attenuation materials for use on small payloads deployed from unmanned aerial vehicles. He derives quantitative relationships among impact shock parameters showing two very important facts. Required cushion thickness is proportional the square of payload’s initial velocity, while material properties determine the deceleration of the payload. He also defines a metric called material crush thickness efficiency to describe the amount of initial cushion thickness required to achieve a certain crush displacement. These quantitative relationships are then used to choose a honeycomb impact attenuator with the proper dynamic crush stress to shield a

---

<sup>\*</sup> Unpublished Work, given to team February 2003.

given payload from an impact shock greater than 30g. Anderson then verifies results by measuring payload deceleration during drop testing.

This 16.62x project builds directly on Anderson’s work, which provides a strong quantitative basis for comparing attenuation properties of expanding foam with honeycomb. A selection of this work can be found in Appendix A. Anderson’s theory coupled with standard drop-test methodologies provide the basis for exploring a novel impact attenuation system for payloads deployed from UAVs.

### 3. Description of Experiment

#### 3.1. Experiment Overview

A flowchart describing the experiment overview is presented in Figure 2. The experiment was divided into two segments and reflects the separation between the primary and secondary hypotheses.

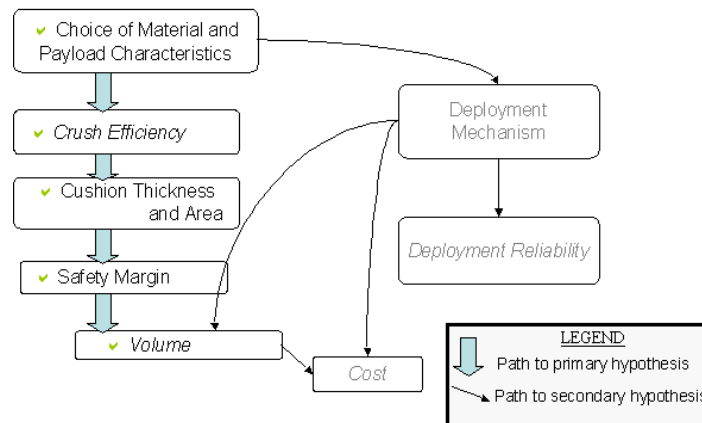


Figure 2: Experiment Overview Flowchart

Once attenuation materials and payload properties were determined, the crush thickness efficiencies were characterized for both honeycomb and expanding foam. The crush thickness efficiency\* is defined as the ratio of the crush displacement of the impact material to its cushion thickness before impact.

\* Definition taken from unpublished work by Chris Anderson entitled, “Impact Shock Attenuation for Parafoil Payloads”

Crush efficiency was measured through quasi-static and dynamic tests. Quasi-static tests involved using a force-press to crush the test materials, and dynamic tests involved dropping payloads of constant mass and constant base area protected by attenuation materials. Dynamic tests were specifically conducted to explore the possibility of velocity-dependent attenuation characteristics not revealed through quasi-static testing.

Drop-tests were then conducted to characterize an adequate cushion safety margin based on a distribution of peak accelerations experienced by the payload during impact. Finally, using this safety margin, pre-deployment volumes were calculated for honeycomb and expanding foam.

This experiment did not include the design and testing of an expanding foam deployment mechanism and thus the secondary hypothesis regarding deployment reliability and cost was not assessed. However, a measure of foam expansion reliability independent of a deployment mechanism was quantified. This foam expansion reliability was compared to the honeycomb deployment reliability. Honeycomb deployment reliability was defined as 100% since honeycomb does not need to be deployed.

## **3.2. Apparatus**

### *3.2.1. Test Setups*

The experiment tests were performed using three distinct test setups.

1. An Instron® force press (at the MIT TELAC laboratories) was used to perform quasi-static load tests of both expanding foam and paper honeycomb. Values of crush thickness efficiency and crush stress were derived from data obtained during these tests.

2. A vertical drop-test rig was built on the strong wall at the MIT Gelb laboratory and is shown in Figure 3. This was used for the dynamic crush thickness efficiency tests of each material and, later on, for safety margin tests to obtain a distribution of the peak accelerations experienced by the payload during impact.



Figure 3: Drop-test Rig

The drop-test rig consisted of two 6 foot high shafts that were held up by two Unistrut® frames and that guided the payload in a vertical descent. The frames, plus a beam holding the pulley from which the payload hung, were clamped to the strong wall. This made it necessary to clamp a 2 inch high platform at the bottom of the test rig such that the line of sight to the attenuation material during impact would not be obstructed by the bottom frame. Finally, the rope wire holding the payload was attached to a quick-release loop and to a winch.

The main function of the shafts was to ensure that the bottom surface of the payload landed horizontally and that the impact attenuation material was crushed evenly. However, friction and a slight outward buckling in the shafts slowed down the payload during its descent. Although time constraints prohibited the implementation of possible solutions, it is likely that impact velocity could have been increased through one or both of the following improvements:

- using ball bearings rather than linear bearings to guide the payload and decrease the friction with the shafts; and
- adding tension to the shafts to unload the compressive force that was causing the shafts to buckle during the descent of the payload.

Pulleys and a quick-release mechanism were necessary such that the payload could be released from a distance, and a winch was used to lift the payload before every drop during the tests.

3. An InstapakQuick Warmer (shown in Figure 4) and four wooden boards comprised the setup for the foam deployment reliability tests. The unexpanded Instapak foam bags were heated for at least thirty minutes and then placed between the four wooden boards, which were clamped together, describing a 5 inch by 12 inch base area. The boards were 5 inches high to allow the foam to expand within this constrained volume.



Figure 4: Instapak Quick Warmer

### 3.2.2. Instrumentation

The instrumentation used to collect data during the tests included the following.

1. The load cell in the MTS Instron force press, which outputs load and displacement of the test material during crush.
2. A high speed camera and its accompanying MIDAS Video Software running on an adjacent computer, in which the attenuation material could be observed frame by frame during crush at 2000Hz. The software facilitated the maximum crush displacement measurement during the dynamic crush efficiency tests. Furthermore, the software, which calculated the velocity of a point between consecutive frames, was used to confirm an impact velocity of  $13.5 \pm 0.3$  feet per second during the safety margin tests.
3. A Crossbow accelerometer was attached to the payload and connected to an analog to digital converter. This signal was recorded using LabView on an adjacent

computer. The accelerometer was used to measure acceleration (shock) during crush for the safety margin tests.

4. Calipers were used to measure the initial cushion thicknesses of every sample of material tested, as well as the post-deployment volume of expanding foam during the reliability tests.

5. The pre-deployment volume of the expanding foam bags was measured by displacing water in a beaker.

### 3.3. Test Articles

The test articles throughout this project were paper honeycomb and expanding foam. These materials were cut to the appropriate dimensions using the band saw in the MIT Gelb laboratory workshop, crushed at the Instron force press for the quasi-static tests, and attached to the bottom of the payload box for drop-tests. Expanding foam was also the test article for the expansion reliability tests. The Instapak expanding foam product used is shown in Figure 1. Hexacomb700™ paper honeycomb, which is manufactured by Pactiv Corporation, is shown in Figure 5.

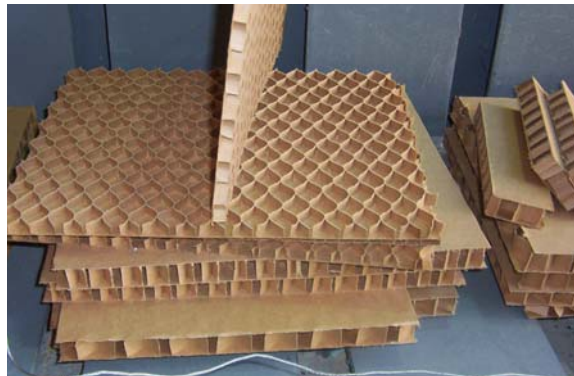


Figure 5: Sliced 1-inch Honeycomb

#### 3.3.1. Paper Honeycomb

All the paper honeycomb samples tested, which were required to be of different thicknesses for different tests, had the same cell sizes to ensure a consistent material behavior during crush. This was an issue during the project because paper honeycomb free samples are only available in discrete thicknesses down to  $\frac{3}{4}$ -inch, which was not thin enough to guarantee that the material would crush completely during the dynamic

crush efficiency tests. This challenge was overcome by slicing in half the 1-inch thick honeycomb samples using the band saw, as can be seen was done for the top samples on Figure 5.

### 3.3.2. Expanding Foam

The Instapak foam was expanded using the setup for the reliability tests. After the bags had been heated, the two chemicals were mixed by alternatively pushing the sacs that contain them inside the bag until these burst and the bag started expanding, as shown in Figure 6. The foam was taken out of the plastic bag before being sliced to the proper dimensions. Since these samples were more irregular than the honeycomb samples, special care was taken to measure the cushion areas and thicknesses of the expanding foam samples to confirm that these met the parameters dictated for each test.



Figure 6: Foam Expansion Procedure

### 3.3.3. Payload Box

The dynamic tests were performed by taping the impact attenuation materials to the bottom of the payload box that was attached to the vertical shafts of the test rig. The box, shown in Figure 7, was built out of 0.7 inch thick plywood and with wooden reinforcements in all inner edges. Each side was glued and then bolted to these reinforcements. The box proved to be sturdy and did not brake or crack during the duration of the drop tests.

The payload mass had to be changed to ensure that each sample, given the material crush stress and the sample area, would crush completely during the dynamic crush efficiency tests. As shown in Figure 7(a), long screws were attached inside the box such that the masses could be bolted down to prevent any safety hazards and mitigate the effects of the mass rebound on the impact acceleration measurements.



Figure 7: (a) Payload Box, (b) Top View of Payload Attached to Drop-test Rig

The linear bearings that were used to attach the payload to the test rig shafts were bolted towards the upper edge of the box so that deviations from a vertical fall would not be exacerbated. Finally, the accelerometer was bolted towards the base of the box to minimize the readout of the payload vibrations after impact. This can be seen in Figure 7(b).

## 4. Description of Tests

### 4.1. Crush Efficiency

#### 4.1.1. Scope

The crush thickness efficiency was defined for this experiment as

$$\eta_t = \frac{x_{crush}}{\tau_{cushion}}, \quad (\text{Eq. 1})$$

where  $x_{crush}$  is the maximum displacement during crush and  $\tau_{cushion}$  is the initial cushion thickness. This parameter gives a measure of how much initial cushion thickness of a certain material is required to achieve the necessary crush displacement during impact. This metric is important because payload volume capacity will be reduced to compensate for the extra attenuation material necessary to achieve the required cushion thickness before impact. Tests conducted in this experiment sought to characterize appropriate crush efficiencies for honeycomb and expanding foam to protect a payload with a 13.5 foot per second vertical descent rate from a 50g impact shock limit. Although the crush efficiencies characterized in this experiment are related to material properties, they do not define a material property of the attenuation material.

#### 4.1.2. Methods

Quasi-static tests to determine crush efficiency were conducted using the Instron force-press and involved loading the attenuation materials with increasing force and monitoring the material displacement. These tests yielded stress versus displacement curves similar to the conceptual figure shown below.

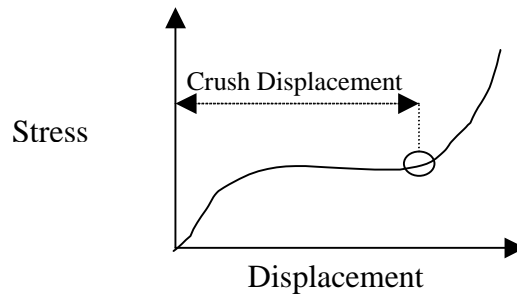


Figure 8: Conceptual Stress vs. Displacement Curve

The crush displacement was defined as the displacement from zero force to the measured displacement where the stress-displacement curve transitions from a plateau to a steep slope. Quasi-static crush efficiency was then determined by taking the ratio of crush displacement to initial cushion thickness.

Dynamic tests involved dropping the payload-attenuation material system from a certain height using less cushioning material than was calculated to be necessary to achieve a deceleration during impact of 50g. This ensured that the attenuation material had completely crushed during impact. Maximum crush displacement of the attenuation material during impact was measured using a high-speed camera. As with quasi-static tests, dynamic crush efficiency was then determined by taking the ratio of crush displacement to initial cushion thickness.

#### 4.1.3. Calibration and Error Mitigation

The high speed camera was calibrated before each testing session by placing a ruler within the camera's field of view to calibrate the camera software's distance and velocity tracking modes. Sampling pictures at 2000Hz and confirming impact velocity after each drop-test mitigated error propagation.

#### *4.1.4. Test Matrices*

The original test matrices developed for this experiment only planned to evaluate static and dynamic crush efficiency for one thickness. However, during the course of testing for honeycomb, a slight discrepancy between quasi-static and dynamic test results indicated that crush efficiency may be a function of initial cushion thickness. Thus, the quasi-static test matrices were expanded for both attenuation materials to characterize a dependence on initial cushion thickness. Unfortunately, the dynamic test matrices could not be expanded to measure crush efficiencies of cushion thickness greater than ½-inch due to a maximum achievable impact velocity of 13.5 feet per second.

Quasi-static crush efficiency for honeycomb was tested for thicknesses of ½, ¾ and 1 inch thick samples. While testing three or more different thickness to characterize expanding foam crush efficiency would have been ideal, mechanical problems with the Instron machine constrained data collection. Ultimately, successful quasi-static tests were conducted for two thicknesses of expanding foam, ½ inch and 1 inch.

Test matrices used for measuring static and dynamic crush efficiencies are shown in Tables 1 and 2 respectively. Quasi-static and dynamic crush efficiencies were measured using the same parameters of attenuation material cushion thickness; the same independent variables of material and trial number, and the same dependent variable of material crush displacement.

Table 1: Quasi-Static Crush Efficiency Test Matrices

Honeycomb			
Thickness			
1/2"			
3/4"			
1"			
Trial Number	Initial Cushion Thickness (inches)	Crush Displacement (inches)	Crush Thickness Efficiency
1-5			
Average			

Expanding Foam			
Thickness			
1/2"			
1"			
Trial Number	Initial Cushion Thickness (inches)	Crush Displacement (inches)	Crush Thickness Efficiency
1-5			
Average			

Table 2: Dynamic Crush Efficiency Test Matrix

Honeycomb & Expanding Foam			
Thickness			
1/2"			
Trial Number	Initial Cushion Thickness (inches)	Crush Displacement (inches)	Crush Thickness Efficiency
1-5			
Average			

## 4.2. Safety Margin

### 4.2.1. Scope

The purpose of characterizing a safety margin is to account for the effect of variations in material properties when determining the necessary pre-deployment volume of an impact attenuator. The tests conducted in this experiment are meant to characterize the variation in material properties of honeycomb and expanding foam under the specific test conditions of 13.5 foot per second impact velocity and 50g impact shock limit. While

slight variations in these test conditions are likely to yield a similar safety margin to the one characterized in this experiment, more testing must be conducted to determine if this safety margin applies to a wide range of test conditions.

#### 4.2.2. *Methods*

Safety margins for honeycomb and expanding foam were characterized by conducting drop-tests using marginal cushion dimensions derived from equations modeling the behavior of the impact attenuators during crush. The equations modeling paper honeycomb are,

$$\tau_{final} = \frac{v^2}{2gG\eta}, \quad (\text{Eq. 2})$$

and,

$$A\sigma_{crush} = mGg, \quad (\text{Eq. 3})$$

where impact velocity ( $v$ ) is 13.5 feet per second, ( $g$ ) is 32.2 feet per second, ( $G$ ) is the deceleration requirement of 50, ( $\eta$ ) is the crush efficiency for the attenuation material being tested, ( $\tau_{final}$ ) is the cushion thickness, ( $A$ ) is the base area of the cushion, and ( $m$ ) is the mass of the payload. However, experiment results indicated that these equations are not a good model for expanding foam. The equations used to model expanding foam are discussed further in the Section 6.4.1.

Twenty-five drop-tests for each material were conducted using marginal cushion dimensions and yielded a distribution of peak accelerations experienced by the payload during impact. From this distribution, new cushion dimensions were chosen to protect the payload within two standard deviations from 50g. These dimensions were found by solving Equations 2 and 3 using the peak acceleration two standard deviations below the 50g impact shock limit.

#### 4.2.3. *Calibration and Error Mitigation*

Much care was taken to mitigate error during the safety margin drop-tests. Acceleration was sampled at 5000 Hz to avoid aliasing. The high-speed camera was calibrated before each drop-test session, and used to confirm that impact velocity was within 0.3 feet per second of 13.5 feet per second. Also, the box was leveled before each

drop test to avoid tilt during impact. High-speed camera images were also used to determine if the box tilted during impact.

#### 4.2.4. Test Matrix

While conducting drop-tests to determine an appropriate safety margin for cushion thickness, the parameters included a fixed height to achieve the desired impact velocity, and the marginal cushion dimensions for each material. The independent variables were material and trial number, and the dependent variable to be measured was maximum acceleration during impact. The test matrix for safety margin calculations is shown in Table 3.

Table 3: Safety Margin Test Matrix

<b>Material: Honeycomb</b>		<b>Material: Expanding Foam</b>	
<u>Trial Number</u>	<u>Maximum Acceleration</u>	<u>Trial Number</u>	<u>Maximum Acceleration</u>
1-25		1-25	

### 4.3. Volume

#### 4.3.1. Scope

The purpose of this measurement is to determine the pre-deployment volume necessary, including safety margin, to protect an 11.5-pound payload with a vertical descent rate of 13.5 feet per second from a 50g impact shock limit.

#### 4.3.2. Methods

The new cushion areas and thicknesses chosen using the safety margin distribution give a measure of the attenuator volume after deployment. Since the volume of honeycomb does not change during deployment, the volume after deployment is also the pre-deployment volume. However, the pre-deployment volume of expanding foam is given by the amount of unexpanded foam necessary to achieve the appropriate attenuator volume after deployment. The pre-deployment volume of expanding foam was given by,

$$V_{ef \text{ pre-deployment}} = \frac{b_{unexpanded} V_{ef \text{ after\_deployment}}}{b_{expanded}}, \quad (\text{Eq. 4})$$

where  $V_{ef\_pre-deployment}$  is the pre-deployment volume of the expanding foam,  $V_{ef\_after\_deployment}$  is the attenuator volume after deployment calculated using the safety margin distribution,  $b_{unexpanded}$  is the volume of an unexpanded bag of expanding foam, and  $b_{expanded}$  is the expected volume of an expanded bag of foam.

#### 4.3.3. Calibration and Error Mitigation

Much of the error in volume measurements are associated with the propagation of error in previous tests, as discussed in the error analysis. Calibration and error mitigation of these tests are discussed in previous sections.

#### 4.3.4. Test Matrix

The pre-deployment volume for honeycomb is evaluated rather than found empirically, and thus is not included in the test matrix. In conducting a test to calculate pre-deployment volume for expanding foam, the independent variable is number of trials. The dependent variable is the volume of water displaced by one unexpanded foam bag. The test matrix for volume measurements is shown in Table 4.

Table 4: Volume Test Matrix

<b>Material: Unexpanded Foam Bag</b>	
<u>Trial Number</u>	<u>Volume</u>
1 -3	

### 4.4. Foam Expansion Reliability

#### 4.4.1. Scope

This test gives a measure of the reliability with which expanding foam will achieve the expected volume specified by the manufacturer within thirty seconds. In this experiment, foam was slowly warmed using the Instapak Quick Warmer. Foam expansion was then manually activated. Warming foam using a device other than

supplied by Instapak may result in a different reliability. Also, this test does not take into account the reliability of a deployment mechanism to activate foam expansion.

#### 4.4.2. *Methods*

Each time a bag of foam was expanded for use in safety margin trials, data was recorded indicating whether the bag successfully expanded to the expected volume within thirty seconds. The expected volume for one expanded bag of foam, as specified by the manufacturer, is 180 cubic inches.

#### 4.4.3. *Calibration and Error Mitigation*

An attempt was made to control the method with which foam was expanded, in order to reduce the effects of outside factors when quantifying foam expansion reliability. Foam was expanded using a consistent method for manually triggering foam expansion. Also, foam was expanded within a barrier constraining area. Finally, all tests were conducted at room temperature and ambient pressure.

#### 4.4.4. *Test Matrix*

The test matrix for foam expansion reliability is shown in Table 5. The independent variable is trial number, and the dependent variable is a Boolean true or false statement for the successful expansion to a cushion volume greater or equal to the expected volume in less than thirty seconds.

Table 5: Foam Expansion Reliability Test Matrix

<u>Trial Number</u>	<u>Successful Deployment</u>
1 - 25	

## 5. Results

The experiment objective involved evaluating expanding foam as an impact attenuation material by comparing several parameters of expanding foam to paper honeycomb. The results displayed in Figure 9 show crush efficiency, pre-deployment volume and expansion reliability of foam as a percent of the same parameters for paper honeycomb. Note that, as stated in the project objective, these results are valid for a

scenario where a payload falling at 13.5 feet per second is protected with a safety margin from an impact shock above 50g.

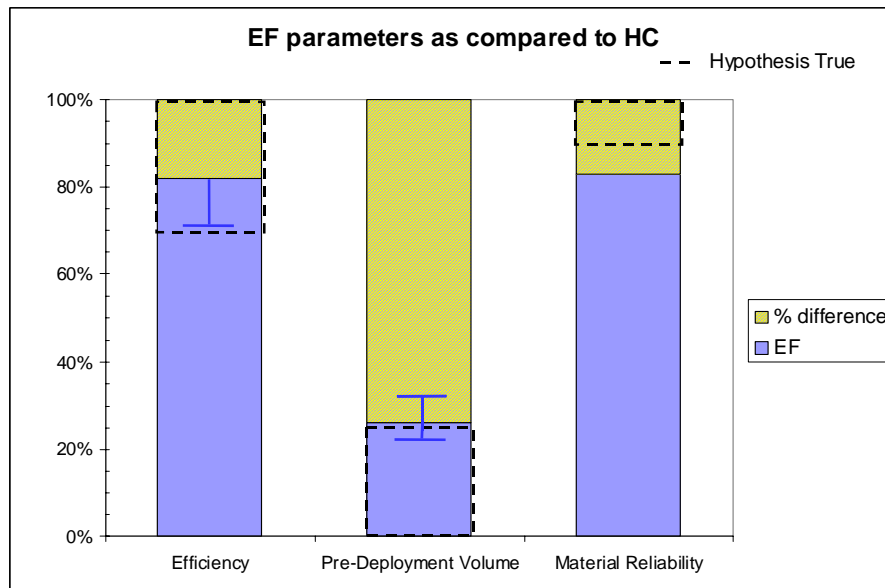


Figure 9: Results of Expanding Foam Comparison to Paper Honeycomb

The dashed boxes in Figure 9 show the range of the hypothesized values for each parameter. The uncertainties associated with the values of crush efficiency and pre-deployment volume, which are discussed in Section 6.7, are depicted by error bars. The results for foam expansion reliability were found with 95% confidence.

It can be seen from this chart that the hypotheses regarding attenuator efficiency and deployment reliability were assessed within experimental error; however, the hypothesis regarding pre-deployment volume could not be proved or disproved. This experiment confirmed that the crush efficiency of expanding foam is at least 70% of the crush efficiency of paper honeycomb, and disproved the hypothesis that the foam expansion reliability is at least 90%.

Overall these results show that, for the scope of this experiment,

- The crush efficiency of expanding foam is at least 72.7% of the crush efficiency of paper honeycomb
- The pre-deployment volume of expanding foam is at most 33.6% the pre-deployment volume of paper honeycomb

- The expanding foam is 83% reliable, with 95% confidence, to expand to its expected volume within 30 seconds.

## 6. Analysis of Results

### 6.1. Analysis of Honeycomb Crush Efficiency Tests

#### 6.1.1. Data Reduction

Crush thickness efficiencies for both honeycomb and expanding foam were derived from the results of quasi-static tests at TELAC and dynamic tests conducted using the drop-test rig. Initial cushion thickness and maximum crush displacement were input into Equation 1 to find the material crush efficiency. The maximum crush displacement was found from the quasi-static stress versus displacement plots as shown for a sample tested in Figure 10, and it was directly observed through the high speed camera for the dynamic tests.

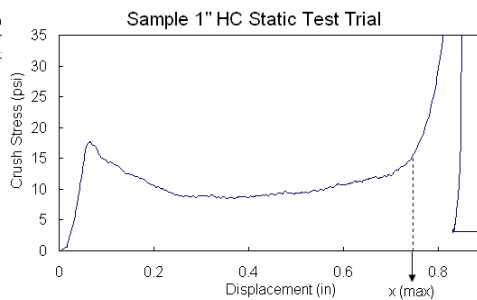


Figure 10: Example of Maximum Crush Displacement

For paper honeycomb, five ½-inch, ¾-inch and 1-inch thick samples were tested at TELAC; while only ½-inch thick samples were tested at the drop-test rig because no higher impact velocities could be met such as to ensure that a thicker sample would be crushed completely.

#### 6.1.2. Discussion of Results

Figure 11 shows the honeycomb crush efficiency results. A trend line fitting the data reveals that crush efficiency is a linear function of initial cushion thickness for the range of thicknesses tested.

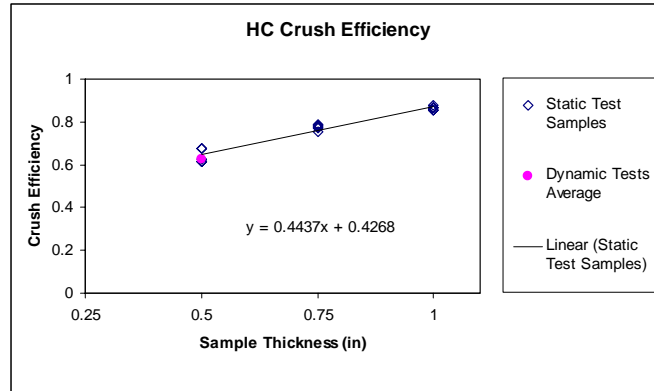


Figure 11: Honeycomb Crush Thickness Efficiency Results

Note that, even though the ½-inch thick samples were sliced and were missing a flat layer of craft paper, the crush thickness efficiencies found for these fit the linear relationship in Figure 11. The sliced samples were therefore considered fair test specimens and used as needed during the experiment. It is also important to note that since the quasi-static and dynamic test results are consistent, velocity dependent attenuation characteristics were discounted.

### 6.1.3. Crush Thickness Efficiency

The purpose of quantifying crush efficiency is to determine the final cushion thickness necessary to protect a payload with the specified vertical descent rate and impact shock limit. While tests showed that crush efficiency is a function of thickness, the objective was particularly concerned with comparing the crush efficiency of expanding foam to paper honeycomb for the cushion thickness dictated by the experiment conditions. In order to be consistent with this objective, it was observed that the final cushion thickness of honeycomb needed to prevent impact shock above 50g is 2.7 inches, as evaluated in final volume calculations. This would require stacking three 1-inch thick samples of honeycomb together, for which the crush thickness efficiency observed would be that of the 1-inch thick samples. Therefore, the final value for honeycomb presented in the results in Section 3 was the average crush thickness efficiency of the five 1-inch thick samples tested at TELAC. This value is 86%.

## 6.2. Analysis of Expanding Foam Crush Efficiency Tests

### 6.2.1. Data Reduction

Quasi-static and dynamic tests were also conducted to characterize the crush thickness efficiency of expanding foam. This time, five 1/2-inch and 1-inch thick samples were tested at TELAC; and only 1/2-inch thick samples were tested at the drop-test rig. However, as will be discussed, it was noted that more crush efficiency measurements would have been necessary to definitively characterize the trend for initial cushion thicknesses greater than one inch.

### 6.2.2. Discussion of Results

Figure 12 shows the quasi-static test results for expanding foam crush efficiency as a function of initial cushion thickness. The trend line fitting the quasi-static data for 1/2 and 1-inch thick expanding foam reveals that crush efficiency is a function of initial thickness for the range of cushion thicknesses tested. Dynamic tests did not yield lower crush efficiencies than measured during the quasi-static tests, so velocity dependent attenuation characteristics were discounted.

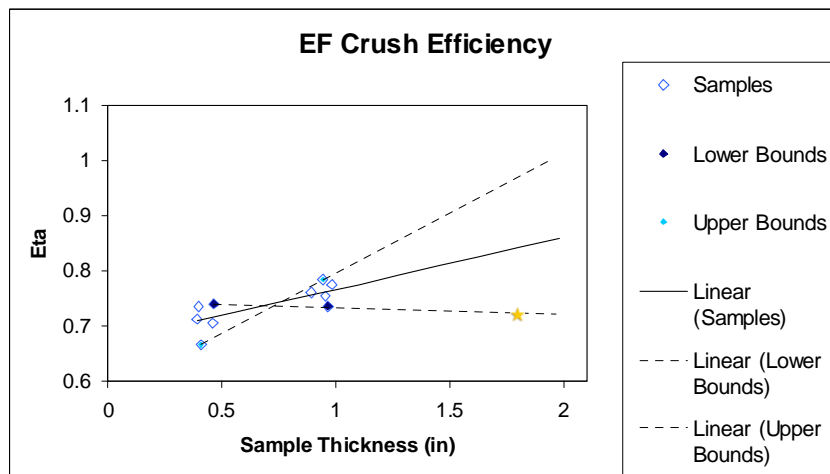


Figure 12: Expanding Foam Crush Thickness Efficiency Results

### 6.2.3. Crush Thickness Efficiency

The expanding foam crush efficiency value concerning this experiment is dependent on the final cushion thickness of material required to protect a payload with the specified vertical descent rate and impact shock limit. The crush displacement

necessary to protect the payload under these conditions was found to be 1.81 inches. This calculation is discussed further in Section 6.4. Because the trend line fitting data for expanding foam crush efficiency as a function of cushion thickness cannot accurately be extended to this initial thickness, upper and lower bounds on crush efficiency were extrapolated. Fitting a trend line to the minimum crush efficiency value at ½-inch and the maximum crush efficiency value at 1-inch created the upper bound. Fitting a trend line to the maximum crush efficiency value at ½-inch and the minimum crush efficiency value at 1-inch created the lower bound.

The lower bound was used to approximate a conservative estimate for crush efficiency which underestimates the expanding foam's true efficiency at this thickness. This step was necessary because no data was collected for larger cushion thicknesses. Underestimating crush efficiency yields an overestimate for cushion thickness, which results in a conservative estimate for pre-deployment volume. Also, extra cushion thickness does not affect the acceleration experienced by the payload during impact since the cushion thickness must be equal to or greater than the crush displacement necessary to slow down the payload. The final result for expanding foam crush thickness efficiency was thus calculated to 72%.

### **6.3. Analysis of Paper Honeycomb Safety Margin Tests**

#### *6.3.1. Data Reduction*

During the safety margin tests, the payload was dropped multiple times and its acceleration as a function of time was recorded during impact. Twenty five test drops for which the impact velocity was confirmed to be  $13.5 \pm 0.3$  feet per second were analyzed. Tests were carried out using an 11.5 pound payload cushioned by 1-inch thick honeycomb with an area of 56 square inches. The accelerometer data for the three Cartesian axes were combined in order to determine the peak absolute acceleration experienced by the payload during impact. Peak accelerations were then plotted as a distribution shown in Figure 13.

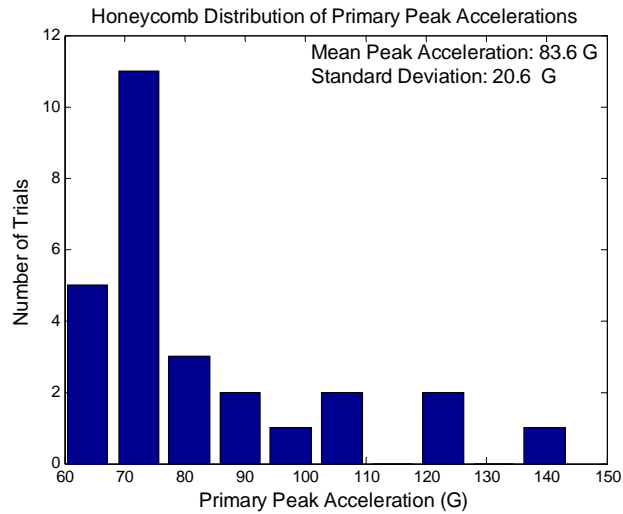


Figure 13: Honeycomb Distribution of Peak Accelerations

The safety margin, defined for the purposes of this experiment as two standard deviations of this distribution, was 41.2g.

The Matlab code used to reduce this data can be found in Appendix B.

### 6.3.2. Data Filtering

The accelerometer data was filtered before being reduced because it showed high frequency vibrations of amplitudes as high as 200g and periods around 1 millisecond, as shown in Figure 14. After a conversation with Professor John Deyst<sup>1</sup>, it was hypothesized that the high frequency data reflected some type of resonance associated with the crushing honeycomb that was left uncharacterized. This resonance was filtered out because it showed very high accelerations that are not associated with the frequency of impact shock of the physical process this experiment was concerned with.

<sup>1</sup> Conversation with Professor John Deyst, November 20, 2003

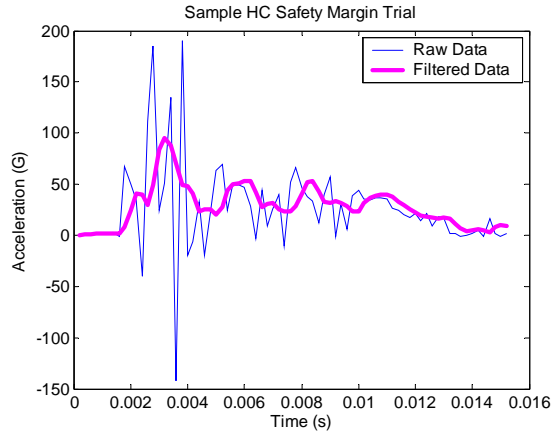


Figure 14: Sample of Filtered Honeycomb Safety Margin Trial

Data was filtered using a low-pass Butterworth filter with a cut-off frequency of 580 Hz. Matlab code for this filter can be found in Appendix B. This cut-off frequency was chosen such that the peak due to buckling seen in the safety margin test data was consistent with the peak stress during seen in the quasi-static loading data obtained at TELAC.

### 6.3.3. Discussion of Results: Comparison to Previous Theory

Safety margin tests were conducted using parameters that were expected to yield a peak distribution with a mean of 50g. As can be seen in Figure 13, the mean peak acceleration was much higher at 83.6g.

This phenomenon can be explained by observing filtered acceleration during impact for each drop-test, which is shown as the bold line in Figure 14. This data reveals two dominant loading modes during impact: the primary peak, which rises up to 95g for this sample, is due to buckling before the honeycomb cells start to collapse; the following peaks of about 50g occur as the cells are collapsing and the material is said to “crush”.

The model used predicted the behavior of honeycomb during crush, but it failed to predict the high peaks observed during buckling. This is because the parameters for the safety margin tests were calculated using Equation 3 and the average value of crush stress for all trials, 10.4 pounds per square inch. The plateau, shown in Figure 15, represents the average crush stress for one trial.

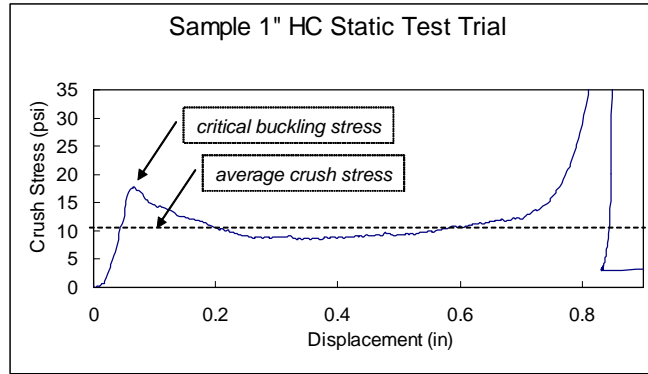


Figure 15: Sample of 1-Inch Honeycomb Quasi-Static Loading Test

This value is the stress on honeycomb as it crushes and after the cells have collapsed. In fact, the mean of the distribution of the secondary peaks in the acceleration versus time plots, which is shown in Figure 16, was within experimental error of 50g, which is the value predicted by our theoretical model.

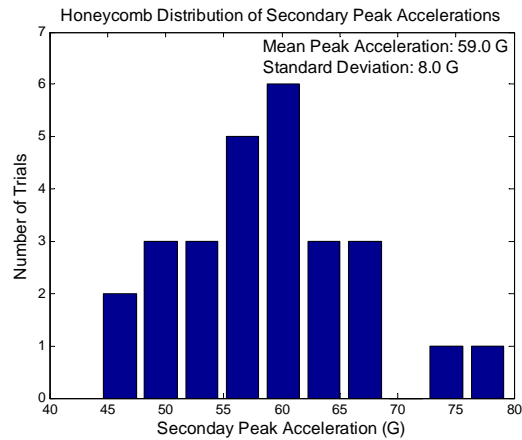


Figure 16: Honeycomb Distribution of Secondary Peak Accelerations

However, since the purpose of impact attenuation is to reduce the *highest* acceleration during impact, the theoretical model was changed to predict buckling rather than crush. The implication of this change is that the stress value used in Equation 3 is now the critical buckling stress rather than the average crush stress. This value, which can also be extracted from quasi-static load test data, corresponds to the initial stress peak before the plateau as seen in Figure 15.

The validity of this modification was readily confirmed by rearranging Equation 3 to find maximum acceleration as a function of buckling stress and the actual parameters

(impact area and payload mass) for which the test was performed. The value of stress input to the equation, 16.4 pounds per square inch, was the average of the critical buckling stresses (as defined above) of the five quasi-static load tests done on 1-inch thick honeycomb samples. The acceleration predicted this time by our model was 79.1g, which matches the mean of the primary peak distribution in Figure 13 within experimental error.

#### *6.3.4. Safety Margin*

The spread of the distribution corresponding to the peak accelerations during buckling was used to characterize a safety margin which would protect a payload from a 50g impact shock limit. The spread corresponding to two standard deviations of the distribution is primarily due to variations in material properties from sample to sample rather than error in impact velocity; this is discussed in more detail in Section 6.7. For honeycomb buckling, two standard deviations was found to be 42.1g. The material properties of honeycomb are not expected to vary greatly whether it is being used to protect a payload from a 50g or 79.1g impact shock limit, especially since the amount material needed for the two shock limits does not differ greatly. Thus the safety margin trials provide an adequate measurement of the safety margin necessary to protect at payload with a 50g impact shock limit to within two standard deviations of the peak acceleration distribution.

### **6.4. Analysis of Expanding Foam Safety Margin Tests**

#### *6.4.1. Analysis of Expanding Foam Crush Stress: Comparison to Previous Theory*

While designing the experiment, expanding foam behavior had been modeled as Anderson modeled paper honeycomb. This model assumed a constant crush stress during crush, and yielded Equation 2 and Equation 3- two decoupled equations governing cushion thickness, cushion area, and acceleration experienced during impact. However, quasi-static tests to quantify expanding foam crush efficiency revealed an interesting and unexpected result: the crush stress of expanding foam during crush is not constant, but is better approximated by a linear function. A graph of crush stress versus crush displacement is shown in Figure 17 below.

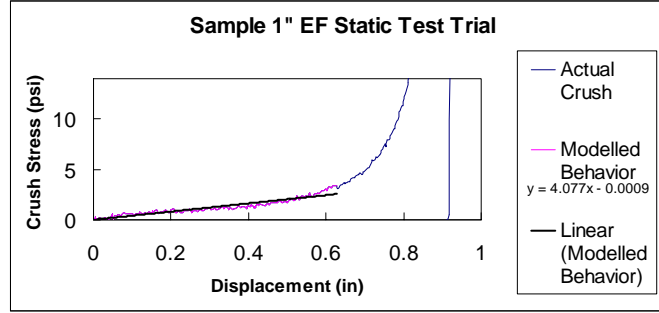


Figure 17: Sample of 1-Inch Quasi-static Loading Test

Modeling expanding foam more accurately as a linear function results in an ordinary differential equation which couples cushion thickness, cushion area, and acceleration experienced during impact. This differential equation is of the form,

$$\ddot{x} + \frac{kA}{m}x = 0, \quad (\text{Eq.5})$$

where (x) is the displacement during crush, (k) is the slope of the crush stress during crush displacement, (A) is the area of the cushion sample, and (m) is the mass of the payload.

This differential equation yields a solution of the form,

$$x(t) = C \sin\left(\sqrt{\frac{kA}{m}}t\right), \quad (\text{Eq. 6})$$

where (C) is an unknown constant representing maximum displacement during crush. Using this form, a relationship between cushion thickness and area can be found by taking the first and second derivatives, and solving for the maximum displacement during crush using impact velocity and the maximum acceleration experienced during impact. The expanding foam initial cushion thickness used to conduct the safety margin tests is then found by dividing the maximum displacement during impact by crush efficiency.

#### 6.4.2. Data Reduction

As with paper honeycomb, the accelerometer data for the three Cartesian axes were combined in order to determine the peak absolute acceleration experienced by the payload during impact. Expanding foam safety margin tests were conducted using the improved model described in Equation 5, which approximated expanding foam crush stress as a linear function of crush displacement. Tests were carried out using an 11.5

pound payload cushioned by 1.81 inch thick expanding foam with an area of 168 square inches. These trials yielded the distribution of peak accelerations shown in Figure 18. The mean of this distribution is 62.2g.

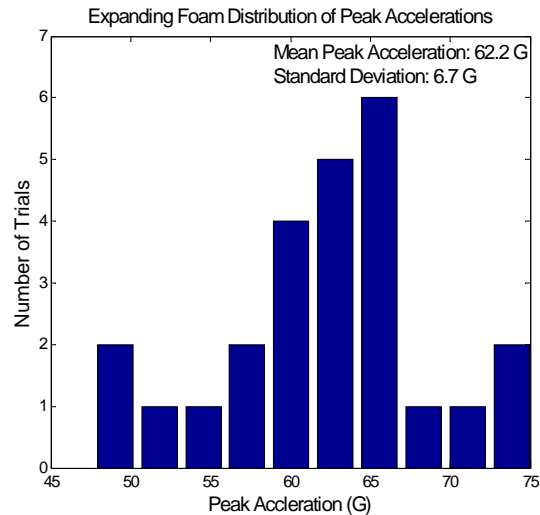


Figure 18: Expanding Foam Distribution of Peak Accelerations

#### 6.4.3. Discussion of Results

While gathering expanding foam safety margin data, observations indicated that most peak accelerations were slightly above the expected 50g; however the results did not seem unreasonable. Later, however, investigation revealed that two parameter errors in our model explained the 12g bias. First, the mass of our payload was specified in Newtons rather than kilograms. Second, the quasi-static data set that was originally used to estimate the slope of the crush stress during crush displacement was erroneous. The data set was determined to be erroneous by comparing the forces exerted by the Instron machine on the expanding foam in this data set and noting a discrepancy when compared to other subsequently collected expanding foam quasi-static data sets and previously collected honeycomb quasi-static data sets.

Interestingly, either one of these parameter errors alone would have resulted in unreasonable peak accelerations during impact and would have immediately flagged an error in the model. For example, the error in mass alone would have resulted in a mean peak acceleration of approximately 21g, while the error in the quasi-static data would have resulted in a mean peak acceleration of approximately 159g. It appears that these

two errors combined to produce reasonable peak accelerations during safety margin trials. When correcting these two parameter errors, inputting the cushion area and thickness used during the safety margin trials, and solving Equation X for peak acceleration, our model yields a mean peak acceleration of 67.0g. This predicted mean is within experimental error of the 62.2g mean found in our safety margin test. Thus, the model of expanding foam is successful at predicting the mean of the peak acceleration distribution.

#### *6.4.4. Safety Margin*

Despite that the distribution of peak accelerations was not centered about 50g, the spread of the distribution was used to characterize a safety margin which would protect a payload from a 50g impact shock limit. This is because the spread corresponding to two standard deviations of the distribution is primarily due to variations in material properties from sample to sample rather than error in impact velocity; this is discussed in more detail in Section 6.7. The value of two standard deviations was found to be 13.4g. The material properties of expanding foam are not expected to vary whether it is being used to protect a payload from a 50g or 62.2g impact shock limit, especially since the amount of expanding foam needed for the two shock limits does not differ greatly. Thus the safety margin trials provide an adequate measurement of the safety margin necessary to protect at payload with a 50g impact shock limit to within two standard deviations of the peak acceleration distribution.

### **6.5. Volume Calculation**

#### *6.5.1. Paper Honeycomb*

A final cushion volume including safety margin was calculated by using an impact acceleration two standard deviations below the impact shock limit of 50g. In this case an impact shock limit of 8.8g was used to solve Equation 3 to determine the base area of paper honeycomb required to protect a payload with an impact shock limit of 50g given a payload mass of 11.5 pounds and a material critical buckling stress of 16.4 pounds per square inch. Equation 2 was then used to determine cushion thickness using the calculated cushion area, an impact velocity of 13.5 feet per second, the crush thickness efficiency of the 1-inch thick samples of honeycomb, and the 8.8g impact shock limit. Using this cushion area and thickness ensure that, 95% of the time, the material adequately protects a payload with a 50g impact shock limit. Note that the

confidence factor was provided by the safety margin incorporated to this equation, as shown in Appendix C. The final cushion volume of honeycomb needed was found to be 27.2 cubic inches.

#### *6.5.2. Expanding Foam*

A final cushion volume including safety margin was calculated by using an impact acceleration two standard deviations below the impact shock limit of 50g. In this case an impact shock limit of 36.6g was used to solve Equation 5 for a cushion area, thickness, and thus volume. This volume was then scaled to a pre-deployment volume based on the volume of an unexpanded Instapak bag using Equation 4. This analysis concluded that, including safety margin, an expanding foam pre-deployment volume of 7.1 cubic inches is necessary to protect a payload from a 50g impact shock limit.

### **6.6. Expanding Foam Reliability Tests**

Out of the twenty five bags of foam expanded for these tests, only one bag expanded to a volume below that expected according to the product specifications. All bags expanded fully within thirty seconds of the chemical mixing. Larson's binomial distribution nomograph<sup>2</sup> was used to plot these results and foam expansion reliability of 83% was found with 95% confidence.

### **6.7. Error Analysis**

The purpose of this analysis is to quantify the error in the measurements of crush displacement efficiency and pre-deployment attenuator volume used to assess our crush efficiency, volume, and reliability hypotheses.

#### *6.7.1. Quasi-Static Crush Efficiency Error*

As discussed in data analysis, dynamic crush efficiencies were not used in the experiment analysis. Thus, these errors do not contribute to the experiment error and are not analyzed in this section.

Crush displacement measurements using an Instron force press are accurate to within 0.01 inches. However, another source of error in measuring crush displacement is the ability to accurately determine the point of inflection in the force versus displacement curve generated by the Instron machine. The error for estimating the inflection point is at most 0.04 inches for honeycomb and at most 0.06 inches for expanding foam. Initial

---

<sup>2</sup> Presented in lecture by Professor John Deyst, November 30, 2003

cushion thickness is measured using a standard ruler with accuracy conservatively estimated to within one-sixteenth of an inch.

Given the equation for crush efficiency (Eq.1) and the general rule for combination of errors:

$$dz = \sqrt{\left(\frac{\delta F}{\delta x_1}\right)^2 dx_1^2 + \left(\frac{\delta F}{\delta x_2}\right)^2 dx_2^2 + \left(\frac{\delta F}{\delta x_3}\right)^2 dx_3^2 \dots} \quad , \quad (\text{Eq. 7})$$

where  $z = F(x_1, x_2, x_3 \dots)$  the error in crush efficiency is given by:

$$d\eta = \eta * \sqrt{\left(\frac{d x}{x}\right)^2 + \left(\frac{d \tau}{\tau}\right)^2} . \quad (\text{Eq. 8})$$

The combined error in honeycomb crush displacement (dx) is 0.041 inches. The initial honeycomb cushion thickness ( $\tau$ ) chosen for our experimental parameters was measured to be 0.946 inches, with an average crush displacement (x) of 0.816 inches. Using these values, Equation (8) yields an error for honeycomb quasi-static crush efficiency of 7.4 %.

The combined error in expanding foam crush displacement (dx) is 0.061 inches. The initial expanding foam cushion thickness ( $\tau$ ) chosen for our experimental parameters was measured to be 2.5 inches, with a crush displacement (x) of 1.81 inches. These values yield an error in expanding foam crush efficiency of 4.2%.

The errors in honeycomb and expanding foam crush efficiency were then normalized to the crush efficiency of honeycomb in order to assess the hypothesis. This normalization resulted in a lower error bound of -11.1% for expanding foam crush efficiency as compared to honeycomb crush efficiency. Because data analysis resulted only in a lower bound on expanding foam crush efficiency, an upper error bound was not quantified.

### 6.7.2. Pre-deployment Attenuator Volume

#### 6.7.2.1. Peak Acceleration Error

Errors in peak acceleration measurements are due to a random accelerometer error and a random error in impact velocity. The peak acceleration measurement error can be used to interpret the experimental data in two ways. First, the error can be used to determine if the mean of the peak acceleration distribution is centered about the expected mean within experimental error. Second, peak acceleration error is propagated to

determine errors in initial cushion thickness, cushion area, and ultimately cushion volume.

For safety margin trials, initial honeycomb cushion thickness was slightly overestimated, and initial expanding foam cushion thickness was slightly overestimated indirectly by underestimating crush efficiency. Because extra cushion thickness does not affect acceleration experienced by the payload during impact, errors in initial cushion thickness and crush efficiency for expanding foam do not affect the errors in peak acceleration measurements. However, errors in crush efficiency, initial cushion thickness, impact velocity and peak acceleration measurements all contribute to error in pre-deployment volume.

Peak acceleration is measured using a Crossbow Accelerometer series CXL100HF3. According to the product specification sheet, the input range is +/- 100g and the sensitivity is +/- 10 millivolts per g. According the specification footnote, this corresponds to a +/- 2% error in the accelerometer measurement. Operating near and around the impact deceleration limit of 50G, this causes a 1G random measurement error.

The experiment was conducted assuming an impact velocity of 13.5 feet per second. Impact velocity was confirmed after each drop-test using a high-speed camera sampling at 1000 frames per second and was found to vary by plus or minus 0.3 feet per second. The instrument error associated with measuring impact velocity with a high speed camera sampling at 1000 frames per second is calculated to be 0.39 feet per second. The general rule for combination of errors yields a total error in impact velocity of 0.49 feet per second. The error in peak acceleration measurement due to the total error in impact velocity is given by:

$$dG = \sqrt{\left(\frac{v}{\eta\tau_{final}}\right)^2 dv^2}, \quad (\text{Eq. 9})$$

where (v) is the average impact velocity of 13.5 feet per second, (dv) is the error in impact velocity, ( $\eta$ ) is the crush efficiency, and ( $\tau_{final}$ ) is the final cushion thickness.

Using the crush efficiency and initial cushion thickness calculated for honeycomb, the error in peak accelerations for honeycomb due to impact velocity error is 8.99g.

Similarly, using the crush efficiency and initial cushion thickness calculated for

expanding foam, the error in peak accelerations for expanding foam due to impact velocity error is 5.01g.

Combining the errors due to the accelerometer measurement and variation in drop-height using the general rule for combination of errors yields an equation for the total error in peak acceleration measurements:

$$dG_{random} = \sqrt{d_{accelerometer}^2 + d_{drop-height}^2} . \quad (\text{Eq. 10})$$

Using Equation (10) yields a total error in peak acceleration measurements for honeycomb of 9.05g, and a total error in peak acceleration measurements for expanding foam of 5.12g.

#### 6.7.2.2. Error in Cushion Dimensions

##### *Honeycomb*

Final honeycomb cushion thickness is calculated using the equation:

$$\tau_{final} = \frac{v^2}{2gG\eta} , \quad (\text{Eq. 11})$$

where (v) is the impact velocity requirement, and (G) is the impact shock limit including safety margin, and ( $\eta$ ) is the crush efficiency, and ( $\tau_{final}$ ) is the cushion thickness including safety margin to protect the payload from accelerations greater than 50g during impact. Using the general rule for combination of errors, the error in the final cushion thickness as a function of the error in crush efficiency and the error in (G) is given by

$$d\tau_{final} = \sqrt{\left(\frac{v^2}{2g\eta(G)^2}\right)^2 dG^2 + \left(\frac{v^2}{2g\eta^2(G)}\right)^2 d\eta^2} , \quad (\text{Eq. 12})$$

where ( $dG$ ) is the error in peak acceleration measurements and ( $d\eta$ ) is the error in crush efficiency. For honeycomb, this yields an error in final cushion thickness of 0.30 inches.

Honeycomb final area is calculated using the following,

$$A\sigma_{crush} = mGg , \quad (\text{Eq. 13})$$

where (m) is the mass of the payload, (G) is the impact shock limit including safety margin, (g) is the acceleration due to gravity, and (A) is the base area of the honeycomb. Using the general rule for combination of errors, the error in the final cushion area as a function of the error in (G) is given by,

$$dA = \sqrt{\frac{m^2 g^2 dG^2}{\sigma_{crush}}} . \quad (\text{Eq. 14})$$

Equation 14 yields an error in cushion area of 0.06 square inches.

The pre-deployment volume for the honeycomb impact attenuation material is then given by:

$$V_{honeycomb} = A \tau_{final} . \quad (\text{Eq. 15})$$

Using the general rule for combination of errors, the error in the final cushion volume as a function of the error in thickness and the error in area is given by:

$$dV_{honeycomb} = \sqrt{A^2 d\tau_{final}^2 + \tau_{final}^2 dA^2} . \quad (\text{Eq. 16})$$

where cushion area ( $A$ ) is 6.17 square inches and cushion thickness ( $\tau_{final}$ ) is 3 inches as was found in the data analysis. The errors in cushion area and thickness yield an error in volume of 2.87 cubic inches, which is an 11% error in the volume of honeycomb.

#### *Expanding Foam*

Expressions relating expanding foam area and cushion thickness, found by solving the differential Equation 5 as described in the data analysis, are expressed below:

$$A = \frac{mG^2 g^2}{kv^2} , \quad (\text{Eq. 17})$$

and,

$$\tau_{final} = \frac{vm^{1/2}}{k^{1/2} A^{1/2} \eta} , \quad (\text{Eq. 18})$$

where ( $k$ ) is the estimated slope of the crush stress, ( $m$ ) is the mass of the payload, ( $G$ ) is the impact shock limit including safety margin, ( $\eta$ ) is the crush efficiency, and ( $v$ ) is the impact velocity.

Using the general rule for combination of errors, the error in the final cushion area as a function of the error in velocity and the error in ( $G$ ) is given by:

$$dA = \sqrt{\left(\frac{2mGg^2}{kv^2}\right)^2 dG^2 + \left(\frac{2mG^2g^2}{kv^3}\right) dV^2} , \quad (\text{Eq. 19})$$

Including errors in peak acceleration measurements and impact velocity, the error in cushion area is 0.0003 square inches.

The error in final cushion thickness as a function of errors in velocity and cushion area is given by,

$$d\tau_{final} = \sqrt{\frac{m}{kA} dv^2 + \frac{0.5v^2 mA}{k} dA^2}, \quad (\text{Eq. 20})$$

and yields a 0.3 inch error in cushion thickness.

As with honeycomb, the error in the final cushion volume as a function of the error in thickness and the error in area is given by:

$$dV_{expanding\_foam} = \sqrt{A^2 d\tau_{final}^2 + \tau_{final}^2 dA^2}. \quad (\text{Eq. 21})$$

where cushion area ( $A$ ) is 48.83 square inches and cushion thickness ( $\tau_{final}$ ) is 2.5 inches as was found in the data analysis. Including the errors in cushion area and thickness yield an error in volume of 14.64 cubic inches, which is a 12.1 % error in the volume of expanding foam. The same percent error value applies to the pre-deployment volume of expanding foam required, which is scaled down linearly.

The errors in honeycomb and expanding foam pre-deployment volume were then normalized to the honeycomb pre-deployment volume in order to assess the hypothesis. This normalization resulted in a lower error bound of -5.4% and an upper error bound of +7.5% for expanding foam pre-deployment volume as compared to honeycomb pre-deployment volume.

## 6.8. Relation of Results to Hypothesis

### 6.8.1. Crush Efficiency

For the scope of this test, an expanding foam crush efficiency of 0.72 was compared to a honeycomb crush efficiency of 0.86. The crush efficiency of expanding foam was found to be 83.8% of the crush efficiency of honeycomb. The errors in expanding foam and honeycomb crush efficiencies, normalized to the crush efficiency of honeycomb, resulted in a lower error bound of -11.1 % on expanding foam crush efficiency as compared to honeycomb crush efficiency. These results proved the hypothesis stating the crush efficiency of expanding foam is no less than 70% of the crush efficiency of honeycomb.

### 6.8.2. *Pre-deployment Volume*

For the scope of this test, an expanding foam pre-deployment volume of 7.11 cubic inches was compared to a honeycomb pre-deployment volume of 27.2 cubic inches. The pre-deployment of expanding foam was found to be 26.1% of the honeycomb pre-deployment volume. The errors in pre-deployment volumes, normalized to the honeycomb pre-deployment volume, resulted in an error of  $-5.4\%$ ,  $+7.5\%$  on expanding foam pre-deployment volume as compared to honeycomb pre-deployment volume. These errors resulted in an uncertain assessment of the pre-deployment volume hypothesis.

### 6.8.3. *Foam Expansion Reliability*

For the scope of this test, expanding foam was found to a foam expansion reliability of 83% with a 95% confidence. Thus, the hypothesis stating that expanding foam had at least 90% reliability was disproved.

## 7. **Conclusions**

### 7.1. **Assessment of Hypothesis**

The hypotheses regarding attenuator efficiency and deployment reliability were assessed within experimental error; however, the hypothesis regarding pre-deployment volume could not be proved or disproved. This experiment confirmed that the crush efficiency of expanding foam is at least 70% of the crush efficiency of paper honeycomb, and disproved the hypothesis that the foam expansion reliability is at least 90%.

### 7.2. **Other Findings**

The results found regarding the hypotheses' metrics were:

- The crush efficiency of expanding foam is at least 72.7% of the crush efficiency of paper honeycomb
- The pre-deployment volume of expanding foam is at most 33.6% the pre-deployment volume of paper honeycomb
- The expanding foam is 83% reliable, with 95% confidence, to expand to its expected volume within 30 seconds.

Other results not directly related to the initial hypotheses included:

- Honeycomb crush efficiency is a function of initial cushion thickness

- Honeycomb buckling, rather than crush, results in peak accelerations experienced by the payload during impact.
- Expanding foam crush stress is not constant during crush displacement, and can be accurately characterized using a linear approximation with positive slope.
- Figure 19 shows that for a given payload mass, impact velocity, and appropriate crush stress characterization:

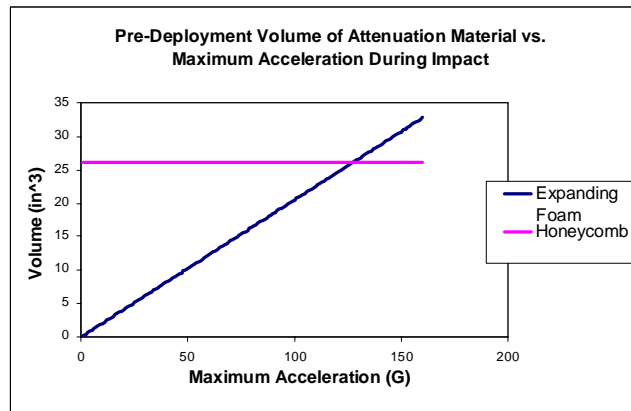


Figure 19: Pre-deployment Volume of Attenuation Material vs. Maximum Acceleration During Impact

- Honeycomb volume is constant for all maximum impact acceleration limits. However areas and thicknesses necessary to protect the payload do vary with maximum impact acceleration limits.
- Expanding foam volume is a linear function of maximum acceleration limit.

### 7.3. Suggestions for Future Work

This experiment formulated models for using honeycomb and expanding foam to protect a payload from experiencing more than a 50g shock during impact within a safety margin. However, due to time constraints, the final cushion dimensions for honeycomb and expanding foam resulting from this experiment were not tested to ensure they do indeed protect the payload adequately. The first recommendation for future work is to conduct drop tests to experimentally verify the results of this experiment. We also recommend that the scope of this project be expanded to study other impact velocities

and shock limit conditions to determine a range of conditions under which it is advantageous to use one attenuation material over another. Finally, we recommend that future work include designing a reliable, low-volume, low-weight mechanism to expand foam onboard an unmanned aerial vehicle.

## **8. References**

1. Gardinerier, D., Yanagihara, M., Kobayashi, T., and Amito, A., "Design and Testing of the HOPE-X HSFD-II Landing System," *AIAA Journal*, Vol. A01-29285, 2001, pp.304-310.
2. Brown, G., Haggard, R., "Parachute Retraction Soft-Landing Systems Using Pneumatic Muscle Actuators," *AIAA Journal*, Vol. A00-37300, 2000, pp.1-9.

## **Acknowledgements**

We would like to thank Chris Anderson; his dedication to us, generosity with his knowledge, and enthusiasm made this project a fantastic experience.

We would also like to express our appreciation for Don Wiener, Dave Robertson, Dick Perdichizzi and John Kane, who were instrumental during the construction and data collection stages of this project.

Finally, we extend our gratitude for the guidance and instruction provided by Professor Deyst, Professor Greitzer, Jennifer Craig.

**Appendix A: Selections of Anderson’s Unpublished Paper**  
**Appendix B: Matlab Code for Safety Margin Tests Data Reduction**  
**Appendix C: Safety Margin Confidence Analysis**  
**Appendix D: Summary of Intermediate Results**

---

<sup>1</sup> Gardinerier, D., Yanagihara, M., Kobayashi, T., and Amito, A., “Design and Testing of the HOPE-X HSF-D-II Landing System,” *AIAA Journal*, Vol. A01-29285, 2001, pp.304-310.

<sup>2</sup> Brown, G., Haggard, R., “Parachute Retraction Soft-Landing Systems Using Pneumatic Muscle Actuators,” *AIAA Journal*, Vol. A00-37300, 2000, pp.1-9.